# Carrier Dynamics in $TiO_2$ and $Pt/TiO_2$ Powders Observed by Femtosecond Time-Resolved Near-Infrared Spectroscopy at a Spectral Region of 0.9−1.5 $\mu$m with the Direct Absorption Method

**Koichi Iwata,*,† Tomohisa Takaya,‡ Hiro-o Hamaguchi,‡ Akira Yamakata,§,|| Taka-aki Ishibashi,§,⊥ Hiroshi Onishi,§,# and Haruo Kuroda⊗**

*Research Centre for Spectrochemistry and Department of Chemistry, School of Science, The University of Tokyo, 7-3-1 Hongo, Bunkyo-ku, Tokyo 113-0033, Japan, Surface Chemistry Laboratory, Kanagawa Academy of Science and Technology (KAST), KSP East 404, 3-2-1 Sakato, Takatsu, Kawasaki, 213-0012, Japan, and IR FEL Research Center, Research Institute for Science and Technology, Tokyo University of Science, Yamazaki 2641, Noda, Chiba 278-8510, Japan*

*Received: June 8, 2004; In Final Form: September 20, 2004*

Femtosecond time-resolved near-infrared spectra of $TiO_2$ and $Pt/TiO_2$ powders are measured at the wavelength region of 0.9−1.5 $\mu$m with the direct absorption method. Broad absorption bands of charge carriers, mainly free and trapped electrons, are observed for $TiO_2$ and $Pt/TiO_2$. The absorption band shape changes with a time constant of 160 fs after the photoirradiation, which most probably reflects the trapping of the generated free electrons. Population decay curves of the carriers after 1 ps, obtained for three different pump light powers, are well-explained by the second-order decay kinetics with a common second-order rate constant, indicating nongeminate recombination of the electron−hole pairs. When Pt is loaded to $TiO_2$, an additional decaying process of 2.3 ps is observed. This decay component represents the transfer of generated electrons from $TiO_2$ to Pt, which is consistent with the known increase of overall catalytic activities by the Pt cocatalyst.

## Introduction

Photocatalytic reactions start when charge carriers are generated upon the photoirradiation. For studying the mechanism of a photocatalytic reaction, it is essential to trace the behaviors of the charge carriers from the moment they are generated. In case of photochemical reactions involving $TiO_2$, which have been studied extensively,[1−3] the carriers either oxidize or reduce reactant molecules on the surface of the $TiO_2$ particles. However, it has not been fully understood how the carriers reach the surface area, how they dissipate the excess energy and get stabilized, how they oxidize or reduce the reactant molecules, or how they migrate to cocatalyst particles such as Pt on $Pt/TiO_2$. When trying to answer these basic questions, it is helpful to trace dynamic behaviors of the charge carriers with direct time-resolved spectroscopic measurements. The methods can give straightforward answers to some of the important questions.

Time-resolved visible absorption spectroscopy, or flash photolysis, is commonly used when the mechanism of a photochemical reaction is studied. There is a difficulty, however, when this method is applied to the photocatalytic reactions on the $TiO_2$ powders. Strong light scattering by the sample particles hinders the direct absorption measurement severely. Therefore, diffuse reflectance spectroscopy has been applied to the scattering powder or suspension samples.[4−11] A pulsed laser output at 620 nm[4−6] or a white light continuum between 400 and 750 nm[7−11] was used as the probe light. Although various kinetic processes have been revealed with the use of femtosecond light sources in these experiments, the time-resolution of the measurements were stretched to a picosecond or longer. Wide distribution of the probe light path lengths, caused by the multiple scattering in the sample, broadened the temporal width of the overall probe pulse. The response function of a diffuse reflectance measurement was estimated by simulating the multiple scattering process.[12,13]

Unlike the powder samples, direct absorption measurements in the visible region are possible with $TiO_2$ colloidal solutions. Time-resolved visible absorption spectra have been recorded with the time resolution of sub-microseconds,[14,15] a few tens of picoseconds,[16,17] or 50 to 200 fs.[3,18−20] In the femtosecond experiments, decay dynamics of the charge carriers have been measured at a single wavelength of 620 nm[5,18,19] or between 650 and 700 nm.[20] Time-resolved absorption spectra of colloidal solutions of ZnCdS and CdS were recorded as well.[21] The femtosecond transient reflecting grating method was applied to the $TiO_2(001)$/KSCN(aq) interface.[22] From these studies, carrier dynamics in the femtosecond time region has been successfully revealed. If femtosecond time-resolved measurements of the powder samples are possible, they will provide important information on the mechanism of many photocatalytic reactions occurring on the powder particle surfaces.

The probability of light scattering is decreased when the wavelength of the light becomes longer. By using the infrared probe light, instead of the visible light, time-resolved spectra

* Corresponding author. E-mail: iwata@chem.s.u-tokyo.ac.jp. Fax: 81 3 3500 6902.
† Research Centre for Spectrochemistry, The University of Tokyo.
‡ Department of Chemistry, The University of Tokyo.
§ Kanagawa Academy of Science and Technology (KAST).
|| Present address: Catalysis Research Center, Hokkaido University, Kita 21, Nishi 10, Kita-ku, Sapporo 001-0021, Japan.
⊥ Present address: Department of Chemistry, Graduate School of Science, Hiroshima University, 1-3-1 Kagamiyama, Higashi-hiroshima, 739-8526, Japan.
# Present address: Department of Chemistry, Faculty of Science, Kobe University, 1-1 Rokkodaicho, Nadaku, Kobe 657-8501, Japan.
○ Professor Haruo Kuroda passed away on May 4, 2004.
⊗ Tokyo University of Science.

10.1021/jp047531k CCC: $27.50 
Published on Web 12/04/2004

of scattering samples can be measured with the direct absorption method. Heimer and Heilweil used picosecond mid-infrared pulses at 5.6−6.0 $\mu$m for monitoring the decay dynamics of electrons in the $TiO_2$ microparticles.[23] Lian and his collaborators used femtosecond pulses in the 5−6 $\mu$m region and observed the electron injection process from the dye molecules to the $TiO_2$ particles.[24−26] Yamakata et al. measured nanosecond time-resolved infrared spectra in the 2.5−12 $\mu$m region and clarified the effect of water, oxygen, and methanol on the charge carrier quenching process.[27−34] We originally used this method for observing the charged carrier dynamics in a polyacetylene film and discussed its mechanism in 1989.[35,36] Although the direct time-resolved absorption measurement in the mid-infrared region is quite informative, it is technically not easy to measure a picosecond or subpicosecond time-resolved infrared spectrum with a wide spectral coverage.

In the near-infrared region, between 0.9 and 2.5 $\mu$m, a few time-resolved spectroscopic measurements on photocatalytic reactions have been performed. Sundström and his collaborators observed the injection and recombination of electrons from a dye molecule adsorbed on $TiO_2$ particles in a colloidal solution[37] or in a thin film in acetonitrile[38] by using femtosecond time-resolved spectroscopy between 400 and 2000 nm. Katoh and his collaborators observed the electron-transfer process from a dye sensitizer to ZnO particles with time-resolved near-infrared spectroscopy in the 1.0−2.8 $\mu$m region.[39,40] They assigned the near-infrared absorption bands measured 1 $\mu$s after the photoexcitation to those of free and trapped electrons and holes.[41] Hannappel et al. reported the femtosecond dynamics of electrons injected to the anatase $TiO_2$ colloidal film observed at a single wavelength of 1.1 $\mu$m.[42] Microsecond time-resolved spectra of dye-sensitized anatase $TiO_2$, for the spectral region of 0.5 to 2.0 $\mu$m, have been reported.[43] For the $TiO_2$ particles, however, there has been no report on femtosecond time-resolved near-infrared spectroscopy, to the best of our knowledge.

In this article, we report femtosecond time-resolved near-infrared spectroscopy of $TiO_2$ and $Pt/TiO_2$ microparticle powders in the wavelength region between 0.9 and 1.5 $\mu$m. In this spectral region, it is possible to record the decay kinetics of photogenerated charge carriers with the direct absorption method, while keeping the time resolution to 120 fs. We observe the relaxation process of 160 fs, which most probably reflects the relaxation of free electrons. Effects of the carrier densities and the Pt loading on the decay dynamics are also examined. For $Pt/TiO_2$, we observe an additional decay component of 2.3 ps. We think that it represents the electron-transfer process from $TiO_2$ to the loaded Pt cocatalyst.

## Materials and Methods

Time-resolved near-infrared spectra were measured with a conventional pump−probe method. Details of the apparatus will be published elsewhere. In short, femtosecond light pulses from a Ti:sapphire regenerative amplifier (780 nm, 1 kHz, 120 fs, 3 mW, Spectra Physics Spitfire) were focused onto a sapphire plate where a white light continuum was generated. The near-infrared portion of the white light was used as the probe light. The second harmonic of the regenerative amplifier output (1 kHz, 2.5−10 mW, 390 nm) was used as the pump light. The beam diameter at the sample was 200 $\mu$m. The probe light that passed the sample placed in the air was analyzed by a spectrograph (Oriel MS127i) and was detected by a linear InGaAs array detector (256 channels, Hamamatsu G8031-256). Fluctuation of the probe light was monitored separately by another set of the spectrograph and the detector. The optical

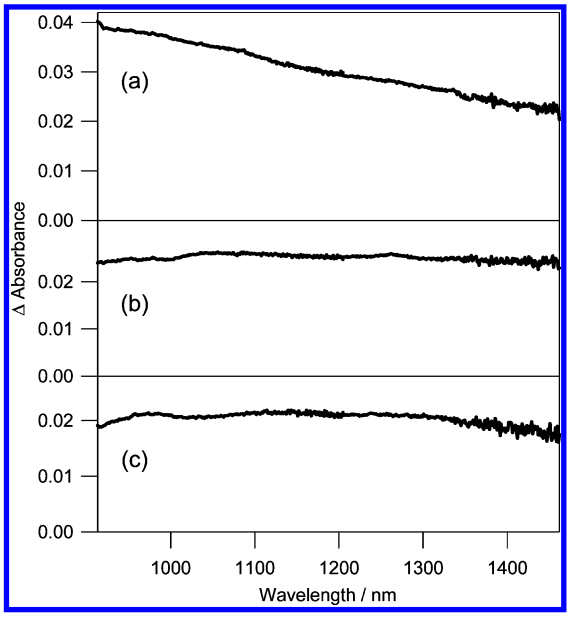


**Figure 1.** Time-resolved near-infrared spectra of photoexcited $TiO_2$ powders measured at 0 fs (a), 400 fs (b), and 10 ps (c) after the photoexcitation at 390 nm. The pump power was 5 mW.

Kerr effect was used for correcting the wavelength-dependent shift of the time origin caused by the group velocity dispersion.[44]

The samples of $TiO_2$ and $Pt/TiO_2$ were prepared as reported in the literature.[27] Powders of $TiO_2$ (TIO4) were supplied from Catalysis Society of Japan. The sample was a mixture of the anatase form and the rutile form (80/20). The average diameter of the $TiO_2$ particles was 20 nm. Platinum (1 wt %) was photochemically deposited on the $TIO_2$ from a $H_2PtCl_6$ aqueous solution. For the spectroscopic measurements, the $TiO_2$ and $Pt/TiO_2$ were fixed on $CaF_2$ plates and heated in air at 573 K to remove organic contaminants.

## Results and Discussion

**Direct Time-Resolved Absorption Measurement of $TiO_2$ Microparticles in the Near-Infrared Region.** The $TiO_2$ photocatalyst particles on a $CaF_2$ plate were irradiated by the 390-nm pump light. The changes induced to the sample by the photoirradiation were monitored with the probe light in the near-infrared wavelength region. A typical set of observed time-resolved near-infrared spectra are shown in Figure 1. The pump light power was 5 mW. In the figure, absorption change induced by the pump light, $\Delta A$, is plotted against the wavelength from 900 to 1500 nm. Although the spectra were recorded at 150 different time delays between −0.7 and 1.2 ps, at 120 delays between −5 and 20 ps, and at 80 delays between −50 and 350 ps, only three representative spectra are presented. Broad absorption features are clearly observed at the time delays of 0 fs (Figure 1a), 400 fs (b), and 10 ps (c).

As mentioned in Introduction, time-resolved absorption measurements of $TiO_2$ have been performed in the visible and mid-infrared regions. To the best of our knowledge, however, no near-infrared time-resolved spectrum in the picosecond to femtosecond time range has been reported.

Because the transient absorption appears immediately after the photoexcitation and because the transient absorption of electrons and holes have been observed in the visible to infrared spectral regions, we think that the transient species that gives absorption in the near-infrared region is either of the electrons or of the holes, or both of them. The steady-state near-infrared absorption spectra of electrochemically reduced colloidal anatase

films,[16,45] chemically reduced rutile crystals,[46] or electrons injected to $TiO_2$ by pulse radiolysis[47−49] show broad and structureless absorption bands, which are similar to the absorption bands shown in Figure 1. Yoshihara et al. estimated the contribution of free electrons, trapped electrons, and trapped holes to the time-resolved absorption spectra between 400 and 2500 nm recorded 1 $\mu$s after the photoexcitation.[41] They concluded that all three species had absorption in the near-infrared region, although the absorption from the holes was flat and smaller than either of the trapped or free electrons. Judging from the reported absorption bands of the electrons and holes, we think that electrons contribute mostly to the transient absorption shown in Figure 1.

In the visible region, a broad absorption band was observed at 2 ps after the photoexcitation of the TIO4 powders by diffuse reflectance measurements.[7,9] The broad absorption band, which covered the whole visible region between 400 and 750 nm, was centered at around 700 nm. This visible absorption band can be naturally connected to the near-infrared absorption band in Figure 1, with a narrow spectral gap of 150 nm. The mid-infrared absorption of charge carriers, observed by the nanosecond time-resolved infrared spectroscopy between 1000 and 3000 $cm^{-1}$, or 10 to 3.3 $\mu$m, shows a monotonic decrease toward the short wavelength direction.[27] The mid-infrared absorption in the nanosecond time region is not simply connected to the present near-infrared absorption band. The electrons injected from coumarin 343 to $TiO_2$ particles gives a flat absorption between 1880 and 2000 $cm^{-1}$ in the picosecond time region.[25] Although there is a large spectral gap between the recorded near-infrared and mid-infrared spectra, it is likely that the carriers show a structureless absorption or reflection at the spectral range covering the visible, near-infrared, and mid-infrared region, at a few picoseconds after the photoirradiation. Free or loosely bound electrons that follow the alternating external electric field without a phase delay reflect the electromagnetic field regardless of its frequency. The structureless absorption or reflection from the visible to the mid-infrared region suggests that the carriers are free or only loosely bound to the opposite charge centers in this condition.

**Carrier Decay Dynamics between 0 and 1 ps.** In Figure 1, two transient species are observed in the near-infrared spectral region. At 0 fs, the observed spectrum shows a negative slope toward the longer wavelength direction, indicating that the absorption maximum is located at the wavelength shorter than 900 nm. The spectral shape is different, however, at 400 fs and 10 ps. The negative slope is not observed any more. The transient species that the gives absorption maximum at the shorter wavelength is absent at 400 fs and later. There are two transient species, one with a lifetime shorter than 400 fs and the other with a lifetime longer than 10 ps.

For analyzing the decay kinetics of the photogenerated charge carriers, time dependence of the absorption change was extracted from the recorded set of time-resolved spectra. In Figure 2, the absorbance changes at 950 (a), 1200 (b), and 1400 nm (c) are plotted against the time delays between −0.5 and 1.2 ps. The pump light power was 5 mW. The observed decay curve at 950 nm is explained well by a combination of a single exponential decay function and a constant offset. The constant component represents a decay process whose time constant is so large that the time dependence appears as a constant offset in this time range. The best fit is obtained when the exponential time constant is 160 fs. The function best fitted to the observed curve is shown in Figure 2a with a dotted curve. When probed at 1400 nm, however, the 160-fs component is absent. Only the

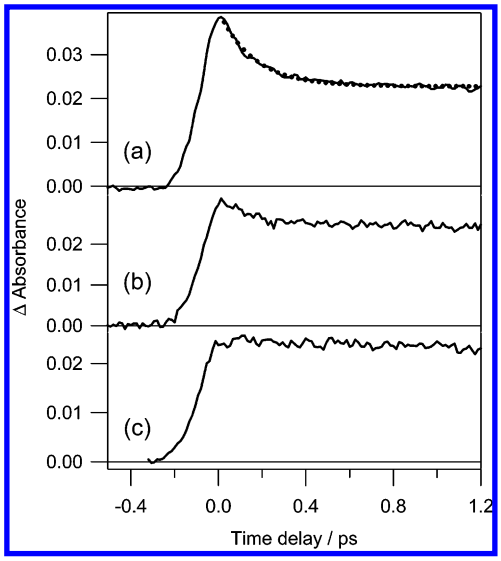


**Figure 2.** Time dependence of the absorption change of photoexcited $TiO_2$ powders measured at 950 (a), 1200 (b), and 1400 nm (c). The pump power was 5 mW. The observed decay curve in part a was best fitted by a combination of a single-exponential decay function with a time constant of 160 fs and a constant offset (dotted curve).

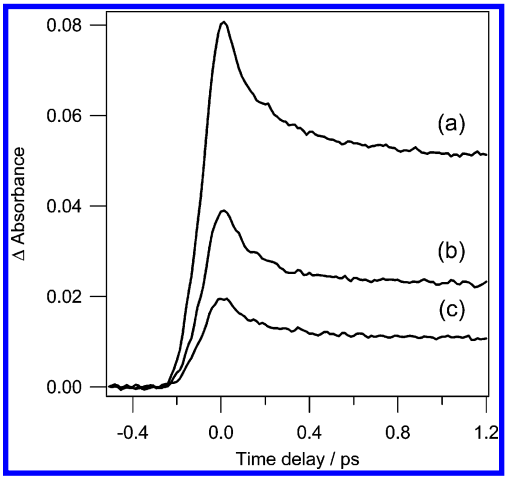


**Figure 3.** Time dependence of the absorption change of photoexcited $TiO_2$ powders measured at 950 nm with the pump power of 10 (a), 5 (b), and 2.5 mW (c). The time delay was changed from −0.5 to 1.2 ps.

constant signals are observed at 1400 nm. At 1200 nm, the amplitude of the 160 fs component is smaller than that at 950 nm. The transient species that has an absorption maximum shorter than 900 nm has a lifetime of 160 fs.

The time profile of the absorbance change at 950 nm was measured at three different pump powers of 10, 5, and 2.5 mW. The results are shown in Figure 3. The fast decaying component of 160 fs and the slow decaying component were observed at all of the pump powers. The ratios between the maximum absorbance change, which includes the contribution from both of the fast and slow decaying components, and the absorbance change at 1.2 ps, which represents the slow decaying component, are 1.6, 1.7, and 1.8 for the pump light powers of 10, 5, and 2.5 mW. Although the density of the generated charge carriers is increased when the pump power is increased, as indicated by the increased amplitude at the time origin, the ratio between the fast decaying component and the slow decaying component remains constant. The relative amplitude of the 160-fs component observed at 950 nm is not affected by the density of the generated charge carriers.

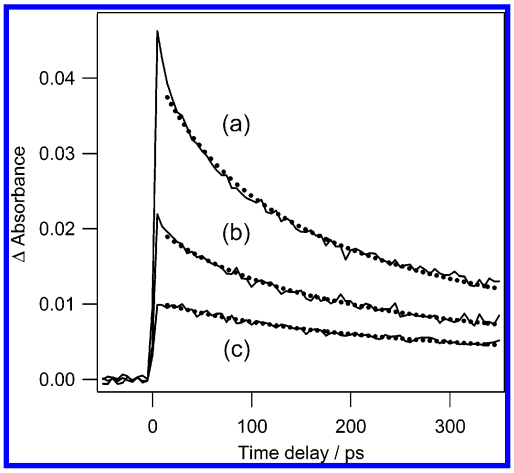


**Figure 4.** Time dependence of the absorption change of photoexcited $TiO_2$ powders measured at 950 nm with the pump power of 10 (a), 5 (b), and 2.5 mW (c). The time delay was changed from −50 ps to 350 ps. The observed decay curves were explained well by a second-order decay kinetics with a common rate constant (dotted curves).

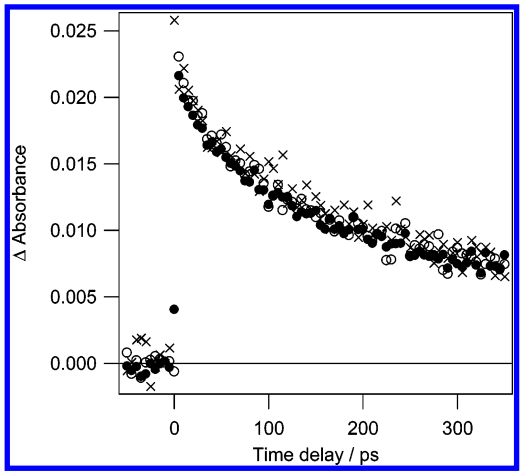


**Figure 5.** Time dependence of the absorption change of photoexcited $TiO_2$ powders measured at 950 nm (●), 1200 nm (○), and 1400 nm (×) with the pump power of 5 mW.

The constant ratio between the fast decaying component and the slow decaying component indicates that the fast decaying process does not involve the interaction with the nearby charge carriers. Most probably, this fast decay represents the trapping process of free electrons. It is also possible that the geminate recombination of the electron and hole pairs contributes to this fast decay. The ordinary geminate recombination, however, simply decreases the signal intensities of the charge carriers. It does not explain the observed change of the spectral shape, at least in a simple way.[50]

The decay time constant of 160 fs agrees with the reported trapping time of photogenerated electrons in colloidal $TiO_2$. The trapping time has been estimated to be 180 fs for 2-nm particles by Skinner et al.[19] and 260 fs for particles whose diameter is assumed to be a few nanometers by Yang and Tamai.[20] The trapping time of the holes has been estimated to be less than 50 fs,[20] indicating the faster motion of holes compared with the electrons. In our experiments, the geminate recombination between the electrons and holes at 160 fs may be difficult, if the holes are trapped at the surface when the electrons are still inside the particles.

As discussed above, the observed spectrum is smoothly connected with the visible absorption band observed 2 ps after the photoexcitation.[7,9] It was suggested that the absorption band in the longer wavelength region was from the trapped electrons. However, our absorption intensity decreases as the wavelength increases, while the spectral shape of the intra-band absorption of the electron has the opposite slope against the wavelength. It is possible that the 160-fs decay represents the relaxation of the exciton state. A decay process of a few picoseconds was observed in the diffuse reflectance measurement of powder $TiO_2$ when the frequency of the pump light matched the band gap energy.[50] It is also possible that the 160-fs component represents the unrelaxed hole, although this is not exactly consistent with the reported trapping time of 50 fs.

**Carrier Decay Dynamics between 1 and 350 ps.** After 1 ps, the charge carriers decay following a different kinetics. The decay kinetics was extracted at 950 nm from the observed time-resolved spectra between −30 and 350 ps for the pump light power of 10, 5, and 2.5 mW. The results are shown in Figure 4 with solid curves. Shapes of the obtained decay curves are quite different depending on the pump light power or the initial density of the generated carriers. In this time range, charge carriers affect the decay process of other charge carriers originated from different electron−hole pairs.

Dependence of the decay curves on the probe wavelength was also examined. The decay curves observed at 950, 1200, and 1400 nm are shown in Figure 5, for the time delays between −30 and 350 ps. The decay curves were identical, regardless of the probe wavelength. This is consistent with the flat absorption spectra observed after 400 fs (Figure 1).

All the observed decay curves in Figure 4 are well-explained, if we assume the second-order decay kinetics with a common rate constant $k_2$ defined in a rate equation,

$$-\frac{dN(t)}{dt} = k_2 N(t)^2 \tag{1}$$

where $N(t)$ represents the number density of the charge carrier at time $t$. In Figure 4, the results of the least-squares fitting analysis are shown with dotted curves. The model function of the fitting was the solution of the second-order rate eq 1. The rate constant $k_2$ was common for all the decay curves. The fitting results are satisfactory.

The second-order decay kinetics shown in Figure 4 represents a nongeminate recombination process between the electrons and holes. In general, relaxation kinetics of the charge carriers should be expressed by the rate equations

$$-\frac{dN_e(t)}{dt} = k_1^e N_e(t) + k_2' N_e(t)\, N_h(t) \tag{2}$$

$$-\frac{dN_h(t)}{dt} = k_1^h N_h(t) + k_2' N_e(t)\, N_h(t) \tag{3}$$

where $N_e(t)$ and $N_h(t)$ represent the number densities of electrons and holes at time $t$. In these equations, nongeminate recombination is expressed by the second-order term whereas other oxidation/reduction or trapping/detrapping processes are expressed as the first-order terms for simplicity. Because the decay signals have been observed in the microsecond time region,[27] the first-order rate, $k_1^e N_e(t)$ and $k_1^h N_h(t)$, should be negligibly slow for the decay kinetics in the picosecond time region. For describing the picosecond kinetics, the eqs 2 and 3 can be written as

$$-\frac{dN_e(t)}{dt} = -\frac{dN_h(t)}{dt} = k_2' N_e(t)\, N_h(t) \tag{4}$$

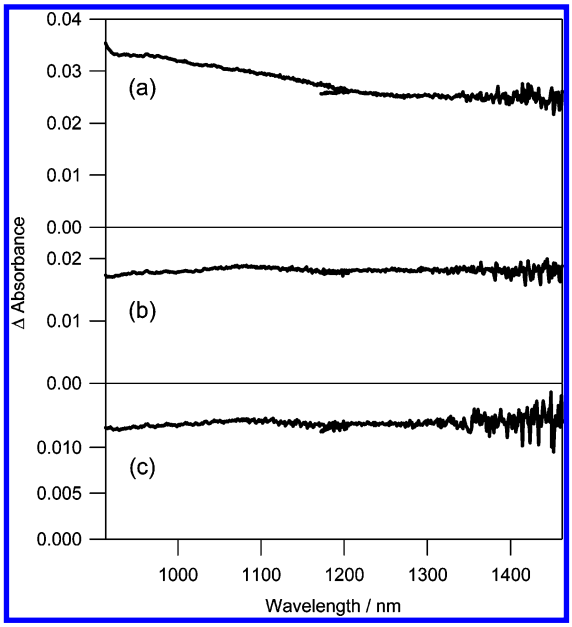


**Figure 6.** Time-resolved near-infrared spectra of photoexcited $Pt/TiO_2$ powders measured at 0 fs (a), 400 fs (b), and 10 ps (c) after the photoexcitation at 390 nm. The pump power was 5 mW.

Because the fast decaying process of 160 fs represents the trapping of charge carriers or geminate recombination of the electron−hole pairs, we can assume that the initial number densities of the electrons and holes for the nongeminate recombination are equal. Therefore, they are equal at an arbitrary time *t*, because the number densities change following the eq 4,

$$N_h(t) = N_e(t) \tag{5}$$

The eq 4 is then rewritten as

$$\frac{dN_e(t)}{dt} = -k_2' N_e(t)^2 \tag{6}$$

which is identical with the eq 1. The decay curves of the charge carriers should follow the second-order decay kinetics with the common rate constant after 1 ps or later, when the fast decaying process is completed. Thus, the observed set of decay curves for three levels of pump power (Figure 4) represents the nongeminate recombination process between the electrons and holes.

**Effect of Pt Loading on Carrier Decay Dynamics.** We compare the carrier dynamics in $TiO_2$ particles loaded by the Pt cocatalyst ($Pt/TiO_2$) with that in $TiO_2$ without Pt, for understanding the mechanism of the improved catalytic activities by the Pt loading. Femtosecond time-resolved near-infrared spectra of $Pt/TiO_2$ were measured with the 390-nm pump light. The results are shown in Figure 6. The observed time-resolved spectra are quite similar to those of $TiO_2$ without Pt (Figure 1). Once again, broad absorption features covering the entire spectral region were observed at the time delays of 0 fs, 400 fs, and 10 ps. An absorption band with the maximum wavelength shorter than 900 nm was observed only at 0 fs.

Time dependence of the absorption change at 1200 nm was extracted from a set of time-resolved near-infrared spectra of $Pt/TiO_2$. The results are shown in Figure 7 (filled circles), together with the results of $TiO_2$ without Pt (open circles), for the time delays of −0.5 to 1.2 ps (a), −4 to 20 ps (b), and −50 to 350 ps (c). The pump power was 5 mW.

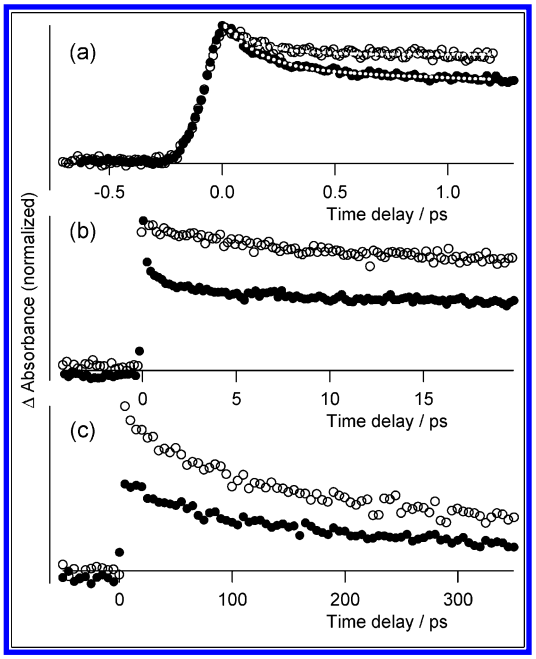


**Figure 7.** Comparison of the decay curves observed at 1200 nm for $TiO_2$ (○) and $Pt/TiO_2$ (●), for the time delays of −0.5 to 1.2 ps (a), −4 to 20 ps (b), and −50 to 350 ps (c). The pump power was 5 mW. The observed curves in part a are well fitted by a single-exponential decay function (160 fs) with a constant offset ($TiO_2$) or by a double exponential decay function (160 fs and 2.3 ps) with a constant offset ($Pt/TiO_2$).

At 10 ps or later, there is little difference observed between the signal decay kinetics of $Pt/TiO_2$ and that of $TiO_2$ (Figure 7c). In this time region, decay kinetics of electrons is not affected by the Pt loading. There is a clear difference observed, however, at the time delays smaller than a few picoseconds (Figures 7a,b). The decay curve observed for $Pt/TiO_2$ has an additional decay component compared with $TiO_2$. Electrons generated in $Pt/TiO_2$ seem to disappear much faster than those in $TiO_2$ do.

The decay curves of $Pt/TiO_2$ and $TiO_2$ are well-explained by exponential decay functions, for the time delays smaller than 1.2 ps. The results of the fitting are shown with dotted curves in Figure 7a. For $TiO_2$, the decay curve was fitted well by the sum of a constant offset and a single exponential decay function with a time constant of 160 fs. The amplitude for the constant offset and the exponential decay was 0.0068 and 0.025. As discussed above, the decay component of 160 fs is most likely to correspond to the trapping of electrons, while the constant component represents the slower nongeminate recombination process. The electron decay process in $Pt/TiO_2$ should involve the same processes observed in $TiO_2$, although the apparent decay curves are different from each other. Therefore, the observed decay curve for $Pt/TiO_2$ was fitted by a combination of a constant offset and two exponential decay functions, one of which had the fixed time constant of 160 fs. The best fit was obtained when the other time constant was 2.3 ps. The amplitudes of the constant offset and the exponential decays of 160 fs and 2.3 ps were 0.012, 0.0096, and 0.0054, respectively.

Photocatalytic activities are improved largely by the Pt loading to the $TiO_2$ particles. The improved catalytic activities in $Pt/TiO_2$ are well-explained if electrons generated by the photoirradiation are transferred to the Pt cocatalyst before they combine with the holes. On Pt, they will have enough time for reducing other reactant molecules. Our experimental results agree with this presumed mechanism. The electron signals disappear faster in $Pt/TiO_2$ than in $TiO_2$ because the electrons are transferred to Pt from $TiO_2$. We think that the decay

component of 2.3 ps, observed only for $Pt/TiO_2$, represents the transfer of generated electrons from $TiO_2$ to the Pt cocatalyst. On the basis of the time-resolved diffuse reflectance measurements with the pump wavelength of 390 nm, Furube et al. have reported the charge separation time between the $TiO_2$ particle (TIO4) and the loaded Pt to be 0.6−5 ps.[10] This is consistent with our result, 2.3 ps, from the direct absorption measurements.

The above interpretation is valid only when the absorption cross section of electrons at 1200 nm is larger in $TiO_2$ than that in Pt. If the Pt cocatalyst holds the metallic characters, it has a half-filled conduction band. Transfer of an electron from $TiO_2$ to Pt increases the number of electrons in the conduction band by one. Because Pt has its plasma frequency in the ultraviolet, the contribution of one electron to the absorption or reflection is spread to a wide spectral range. It is likely that the band intensity for one electron at a single near-infrared wavelength is smaller in Pt than in $TiO_2$.

Although we observe the 2.3-ps decaying component for $Pt/TiO_2$, there remains considerable signal intensity even after hundreds of picoseconds (Figure 7). It is not probable that all the electrons are transferred to the Pt cocatalyst. A portion of the generated electrons should remain in the $TiO_2$ particle. It is also possible that the observed signals have contributions from the holes in addition to the electrons.

In the $TiO_2$ colloidal system, the observed trapping time of electrons and holes was compared with the time required for the carriers to be transferred from the particle interior to the surface.[19,20] The transfer time was estimated from the diffusion coefficients of the electrons and holes. The average diffusion time, or the transit time, from the interior to the surface is

$$\tau = \frac{r_0^2}{\pi^2 D} \tag{7}$$

where $r_0$ is the radius of the particle and $D$ is the diffusion coefficient.[51] Because the diffusion coefficient of electrons in ordinary $TiO_2$ (anatase) has been estimated to be $1 \times 10^{-6}$ $m^2$ $s^{-1}$,[52] the transit time should be 10 ps if $r_0$ is 10 nm, which is the average radius of the present sample. If $\tau$ is equal to 2.3 ps, as is observed, the radius should be 4.9 nm, instead of 10 nm. Apparently, agreement between the observed and estimated transfer times is not poor, considering the simplicity of the diffusion model used for the estimation.

If the observed time constant for the fast relaxation, 160 fs, represents the trapping process of electrons at the surface, then the kinetics is not consistent with the simple diffusion model. It should take 10 ps on average for the generated electrons to reach the surface by diffusion. They cannot be trapped at the surface by 160 fs. There are two possibilities for accounting for the apparent contradiction. First, the electron migration to the particle surface may be much faster than diffusion in ordinary crystals. In this case, electrons reach the surface and are trapped there in 160 fs. There should be then an energy barrier for the electron transfer from the $TiO_2$ to Pt, which proceeds in 2.3 ps. Second, electrons may be trapped inside the particle as well as on the surface. Currently, we do not have enough information for deciding which of the two is the case. We should know the detailed structure of the 20-nm crystal that we study and the behavior of electrons there.

**Advantage of Femtosecond Time-Resolved Near-Infrared Spectroscopy Applied to Scattering Samples.** It is now clear that we can measure femtosecond time-resolved spectra of $TiO_2$ powders with the probe light in the near-infrared region, where light scattering is reduced substantially. In the visible region, diffuse reflectance spectroscopy is used for time-resolved measurements of the scattering samples. Although various dynamic behaviors of charge carriers have been revealed with this method,[4−11] time-resolution of the measurement is determined by the distribution of the probe light path lengths originating from the multiple scattering. Typically, time resolution is limited to a few picoseconds even if femtosecond light pulses are used as the light source.

It is possible to measure picosecond or femtosecond time-resolved absorption spectra of powder samples with the probe light in the mid-infrared region. This method has been successfully applied to the $TiO_2$ samples.[23−26] At present, however, the spectral coverage of the mid-infrared probe light is limited compared with the near-infrared measurement. In the near-infrared, a continuous probe light with a wide spectral coverage and multichannel detectors are readily available, which is still not the case for the mid-infrared. Detector noises in the near-infrared are smaller than those in the mid-infrared. When the time-resolved measurements in the near-infrared and mid-infrared regions provide same information, it is technically easier to use the time-resolved near-infrared spectroscopy.

## Conclusions

We observe the initial processes of photocatalytic reactions proceeding in powder $TiO_2$, by using femtosecond time-resolved near-infrared spectroscopy with the spectral coverage of 900−1500 nm. Unlike the visible region, the direct absorption measurement is possible with the near-infrared probe light. The dynamic behavior of charge carriers generated by the photoirradiation is successfully recorded.

The observed decay kinetics of the charge carriers is well explained by the sum of two different mechanisms. At the time delays between 0 and 1.2 ps, a single exponential decay process with a time constant of 160 fs is observed. The relative amplitude of this component is independent of the pump power or the initial densities of the charge carriers. This fast decay probably represents the trapping of free electrons. After the fast process is completed, the decay curves recorded with three levels of pump power are explained by the second order decay kinetics with a common rate constant. The nongeminate recombination between the electrons and holes is a dominant decay path in this time region. The observed structureless absorption (or reflection) in the near-infrared region, together with the structureless absorption reported in the visible and mid-infrared regions, suggests that the carriers are free or only loosely bound to the opposite charge centers in $TiO_2$.

The generation and decay of the charge carriers are recorded also in the $TiO_2$ particles loaded with the Pt cocatalyst, or $Pt/TiO_2$. In addition to the 160 fs single-exponential decay and the nongeminate recombination observed for $TiO_2$, a decay process of 2.3 ps is observed in $Pt/TiO_2$. We think this component represents the transfer of electrons from $TiO_2$ to Pt.

**Acknowledgment.** This work is supported by Grant-in-Aids for Creative Scientific Research (No. 11NP0101) and Scientific Research (B; No. 15350005) from Japan Society for the Promotion of Science and a Grant-in-Aid for Scientific Research on Priority Areas (Area 417, No. 15033219) from the Ministry of Education, Culture, Sports, Science and Technology (MEXT) of the Japanese Government. K.I. is a recipient of research grants from The Morino Foundation and The Kurata Memorial Hitachi Science and Technology Foundation.

## References and Notes

(1) Fujishima, A.; Honda, K. *Nature* **1972**, *238*, 27.
(2) Kamat, P. V. *Chem. Rev.* **1993**, *93*, 267.

(3) Fox, M. A.; Dulay, M. T. *Chem. Rev.* **1993**, *93*, 341.
(4) Colombo, D. P.; Bowman, R. M. *J. Phys. Chem*. **1995**, *99*, 11752.
(5) Colombo, D. P.; Bowman, R. M. *J. Phys. Chem.* **1996**, *100*, 18445.
(6) Ohtani, B.; Bowman, R. M.; Colombo, D. P.; Kominami, H.; Noguchi, H.; Uosaki, K. *Chem. Lett*. **1998**, 579.
(7) Furube, A.; Asahi, T.; Masuhara, H.; Yamashita, H.; Anpo, M. *Chem. Lett.* **1997**, 735.
(8) Asahi, T.; Furube, A.; Masuhara, H. *Chem. Phys. Lett.* **1997**, *275*, 234.
(9) Furube, A.; Asahi, T.; Masuhara, H.; Yamashita, H.; Anpo, M. *J. Phys. Chem. B* **1999**, *103*, 3120.
(10) Furube, A.; Asahi, T.; Masuhara, H.; Yamashita, H.; Anpo, M. *Chem. Phys. Lett.* **2001**, *336*, 424.
(11) Furube, A.; Asahi, T.; Masuhara, H.; Yamashita, H.; Anpo, M. *Res. Chem. Intermed.* **2001**, *27*, 177.
(12) Asahi, T.; Furube, A.; Fukumura, H.; Ichikawa, M.; Masuhara, H. *Rev. Sci. Instrum.* **1998**, *69*, 361.
(13) Furube, A.; Asahi, T.; Masuhara, H. *Jpn. J. Appl. Phys., Part 1* **1999**, *38*, 4236.
(14) Bahnemann, D.; Henglein, A.; Lilie, J.; Spanhel, L. *J. Phys. Chem.* **1984**, *88*, 709.
(15) Bahnemann, D. W.; Hilgendorff, M.; Memming, R. *J. Phys. Chem. B* **1997**, *101*, 4265.
(16) Rothenberger, G.; Fitzmaurice, D.; Gratzel, M. *J. Phys. Chem.* **1992**, *96*, 5983.
(17) Arbour, C.; Sharma, D. K.; Langford, C. H. *J. Phys. Chem.* **1990**, *94*, 331.
(18) Colombo, D. P.; Roussel, K. A.; Saeh, J.; Skinner, D. E.; Cavaleri, J. J.; Bowman, R. M. *Chem. Phys. Lett.* **1995**, *232*, 207.
(19) Skinner, D. E.; Colombo, D. P.; Cavaleri, J. J.; Bowman, R. M. *J. Phys. Chem.* **1995**, *99*, 7853.
(20) Yang, X. J.; Tamai, N. *Phys. Chem. Chem. Phys.* **2001**, *3*, 3393.
(21) Kaschke, M.; Ernsting, N. P.; Muller, U.; Weller, H. *Chem. Phys. Lett.* **1990**, *168*, 543.
(22) Morishita, T.; Hibara, A.; Sawada, T.; Tsuyumoto, I. *J. Phys. Chem. B* **1999**, *103*, 5984.
(23) Heimer, T. A.; Heilweil, E. J. *J. Phys. Chem. B* **1997**, *101*, 10990.
(24) Asbury, J. B.; Hao, E. C.; Wang, Y. Q.; Lian, T. Q. *J. Phys. Chem. B* **2000**, *104*, 11957.
(25) Ghosh, H. N.; Asbury, J. B.; Lian, T. Q. *J. Phys. Chem. B* **1998**, *102*, 6482.
(26) Ghosh, H. N.; Asbury, J. B.; Weng, Y. X.; Lian, T. Q. *J. Phys. Chem. B* **1998**, *102*, 10208.
(27) Yamakata, A.; Ishibashi, T.; Onishi, H. *Chem. Phys. Lett.* **2001**, *333*, 271.
(28) Yamakata, A.; Ishibashi, T.; Onishi, H. *J. Phys. Chem. B* **2001**, *105*, 7258.
(29) Yamakata, A.; Ishibashi, T.; Onishi, H. *J. Phys. Chem. B* **2002**, *106*, 9122.
(30) Yamakata, A.; Ishibashi, T.; Onishi, H. *Bull. Chem. Soc. Jpn*. **2002**, *75*, 1019.
(31) Yamakata, A.; Ishibashi, T.; Onishi, H. *Chem. Phys. Lett*. **2003**, *376*, 576.
(32) Yamakata, A.; Ishibashi, T.; Onishi, H. *J. Mol. Catal. A* **2003**, *199*, 85.
(33) Yamakata, A.; Ishibashi, T.; Onishi, H. *Int. J. Photoenergy* **2003**, *5*, 7.
(34) Yamakata, A.; Ishibashi, T. A.; Onishi, H. *J. Photochem. Photobiol., A* **2003**, *160*, 33.
(35) Iwata, K.; Hamaguchi, H. *Chem. Phys. Lett.* **1989**, *157*, 300.
(36) Iwata, K.; Hamaguchi, H. *Appl. Spectrosc.* **1990**, *44*, 1431.
(37) Hilgendorff, M.; Sundström, V. *J. Phys. Chem. B* **1998**, *102*, 10505.
(38) Benko, G.; Hilgendorff, M.; Yartsev, A. P.; Sundström, V. *J. Phys. Chem. B* **2001**, *105*, 967.
(39) Katoh, R.; Furube, A.; Hara, K.; Murata, S.; Sugihara, H.; Arakawa, H.; Tachiya, M. *J. Phys. Chem. B* **2002**, *106*, 12957.
(40) Yoshihara, T.; Katoh, R.; Furube, A.; Murai, M.; Tamaki, Y.; Hara, K.; Murata, S.; Arakawa, H.; Tachiya, M. *J. Phys. Chem. B* **2004**, *108*, 2643.
(41) Yoshihara, T.; Katoh, R.; Furube, A.; Tamaki, Y.; Murai, M.; Hara, K.; Murata, S.; Arakawa, H.; Tachiya, M. *J. Phys. Chem. B* **2004**, *108*, 3817.
(42) Hannappel, T.; Burfeindt, B.; Storck, W.; Willig, F. *J. Phys. Chem. B* **1997**, *101*, 6799.
(43) van't Spijker, H.; O'Regan, B.; Goossens, A. *J. Phys. Chem. B* **2001**, *105*, 7220.
(44) Yamaguchi, S.; Hamaguchi, H. *Appl. Spectrosc.* **1995**, *49*, 1513.
(45) Cao, F.; Oskam, G.; Searson, P. C.; Stipkala, J. M.; Heimer, T. A.; Farzad, F.; Meyer, G. J. *J. Phys. Chem.* **1995**, *99*, 11974.
(46) Breckenridge, R. G.; Hosler, W. R. *Phys. Rev.* **1953**, *91*, 793.
(47) Dimitrijevic, N. M.; Saponjic, Z. V.; Bartels, D. M.; Thurnauer, M. C.; Tiede, D. M.; Rajh, T. *J. Phys. Chem. B* **2003**, *107*, 7368.
(48) Safrany, A.; Gao, R. M.; Rabani, J. *J. Phys. Chem. B* **2000**, *104*, 5848.
(49) Dimitrijevic, N. M.; Savic, D.; Micic, O. I.; Nozik, A. J. *J. Phys. Chem.* **1984**, *88*, 4278.
(50) Noguchi, H.; Ohtani, B.; Uosaki, K. Presented at 217th American Chemical Society National Meeting, Anaheim, CA, 1999.
(51) Gratzel, M.; Frank, A. J. *J. Phys. Chem*. **1982**, *86*, 2964.
(52) Enright, B.; Fitzmaurice, D. *J. Phys. Chem.* **1996**, *100*, 1027.